TISSUE ENGINEERING: Part A
Volume 24, Numbers 3 and 4, 2018

DOI: 10.1089/ten.tea.2017.0042

termis
Tissue Engineering
& Regenerative Medicine
International Society

ORIGINAL ARTICLE

Structural Heteropolysaccharide Adhesion to the Glycocalyx of Visceral Mesothelium

Andrew B. Servais, MD,[1] Arne Kienzle, MD,[1] Cristian D. Valenzuela, MD,[1] Alexandra B. Ysasi, BS,[1] Willi L. Wagner, MD,[1,2] Akira Tsuda, PhD,[3] Maximilian Ackermann, MD,[2] and Steven J. Mentzer, MD[1]

Bioadhesives are biopolymers with potential applications in wound healing, drug delivery, and tissue engineering. Pectin, a plant-based heteropolysaccharide, has recently demonstrated potential as a mucoadhesive in the gut. Since mucoadhesion is a process likely involving the interpenetration of the pectin polymer with mucin chains, we hypothesized that pectin may also be effective at targeting the glycocalyx of the visceral mesothelium. To explore the potential role of pectin as a mesothelial bioadhesive, we studied the interaction of various pectin formulations with the mesothelium of the lung, liver, bowel, and heart. Tensile strength, peel strength, and shear resistance of the bioadhesive-mesothelial interaction were measured by load/displacement measurements. In both high-methoxyl pectins (HMP) and low-methoxyl pectins, bioadhesion was greatest with an equal weight % formulation with carboxymethylcellulose (CMC). The tensile strength of the high-methoxyl pectin was consistently greater than low-methoxyl or amidated low-methoxyl formulations ($p < 0.05$). Consistent with a mechanism of polymer-glycocalyx interpenetration, the HMP adhesion to tissue mesothelium was reversed with hydration and limited by enzyme treatment (hyaluronidase, pronase, and neuraminidase). Peel and shear forces applied to the lung/pectin adhesion resulted in a near-interface structural failure and the efficient isolation of intact en face pleural mesothelium. These data indicate that HMP, in an equal weight % mixture with CMC, is a promising mesothelial bioadhesive for use in experimental and therapeutic applications.

Keywords: pectin, mesothelium, adhesion, glycocalyx

Introduction

BIOPOLYMERS, INCLUDING POLYSACCHARIDES, polypeptides, and polyaromatics,[1] are of significant interest in tissue engineering, wound healing, and drug delivery. Biopolymers have the advantages of being abundant, biocompatible, biodegradable, and chemically diverse. Particularly abundant in nature, polysaccharides, composed of monosaccharides that are joined together by glycosidic bonds,[2] have the additional advantage of resembling the glycosaminoglycan molecules in the extracellular matrix of mammalian tissues.[3]

Naturally occurring polysaccharides used in tissue engineering applications include alginate,[4] agarose,[5] cellulose,[6] chitin,[7] and pectin.[8] Pectin is a structural heteropolysaccharide that comprises ~30% of the primary cell walls of plants.[9] Pectin consists mainly of esterified D-galacturonic acid residues in (1 → 4) chains.[10,11] When exposed to calcium, pectin forms egg box-like structures that facilitate the immobilization of substances within the gel structure.[12] Pectin also has the interesting property of being a bioadhesive. The bioadhesivity of pectin, combined with the ability to trap drugs or growth factors within the gel structure, has led to considerable interest in using pectin to target drug delivery[13] as well as to facilitate wound healing.[14]

Pectin's ability to bind nasal and gut mucosa (mucoadhesion) suggests a more general property of pectin as a bioadhesive. Although the mechanism of mucoadhesion is poorly understood,[15] the first step in the process is intimate contact between the mucoadhesive and the mucosa. This wetting phase increases the contact area between the surfaces. The second phase involves the interpenetration of the branched polymers. The interpenetrated chains interact, forming entanglements as well as chemical bonds and weak chemical interactions. A particularly attractive feature of these bioadhesive interactions is the potential for reversibility, that is, the potential for hydration to readily

[1]Laboratory of Adaptive and Regenerative Biology, Brigham and Women's Hospital, Harvard Medical School, Boston, Massachusetts.
[2]Institute of Functional and Clinical Anatomy, University Medical Center of the Johannes Gutenberg-University, Mainz, Germany.
[3]Molecular and Integrative Physiological Sciences, Harvard School of Public Health, Boston, Massachusetts.

disentangle the branched polymers with little adverse effect on the underlying epithelial monolayer.

In addition to gut mucosa, visceral mesothelium is an appealing target for pectin bioadhesion. Mesothelium is the surface layer to serosal tissues of the pleura, pericardium, peritoneum, and tunica vaginalis. Mesothelium is covered by a glycocalyx that functions to limit fluid loss[16] and minimize frictional forces.[17] In this article, we studied the bioadhesion of pectin to the surface glycocalyx of the lung, liver, bowel, and heart mesothelium. The adhesive strength of pectin to the mesothelial glycocalyx was sufficient to not only establish selective interfacial adhesion but also permit the intact isolation of the visceral pleural mesothelium.

Materials and Methods

Animals

Male mice, 8- to 10-week-old wild-type C57BL/6 (Jackson Laboratory, Bar Harbor, ME), were anesthetized before euthanasia.[18] The care of the animals was consistent with guidelines of the American Association for Accreditation of Laboratory Animal Care (Bethesda, MD) and approved by our Institutional Animal Care and Use Committee.

Scanning electron microscopy

The specimen was fixed by immersion in 2.5% buffered glutaraldehyde. After coating with 20–25 Å gold in an argon atmosphere, the mesothelial layer was imaged by using a Philips XL30 ESEM scanning electron microscope (Philips, Eindhoven, Netherlands) at 15 KeV and 21 μA. Stereo pair images were obtained by using a tilt angle difference of 6° on a eucentric sample holder by using standardized processing.

Transmission electron microscopy

Lungs designated for microscopy were harvested after cannulation of the trachea. The tissue was fixed by instillation of 2.5% buffered glutaraldehyde into the bronchial system followed by the instillation of 50% O.C.T. Tissue-Tek (Fisher Scientific, Schwerte, Germany) in saline. Postfixation samples of the lung were embedded in Epon (Serva, Heidelberg, Germany); 700 Å ultrathin sections were analyzed by using a Leo 906 digital transmission electron microscope (Leo, Oberkochen, Germany).

Lectin

Mesothelial staining was performed with Lycopersicon esculentum lectin (LEL). Derived from the common tomato, the lectin bound oligosaccharides of N-acetyl-D-glucosamine specificity.[19] The biotinylated lectin was obtained from Vector Laboratories (Burlingame, CA).

Lectin histochemistry

Cryostat sections were obtained from lung, liver, bowel, and heart specimens; embedded in O.C.T. compound; and snap frozen. After warming the slide to 21°C, the sections were fixed for 10 min (2% paraformaldehyde and phosphate-buffered saline [PBS] at pH 7.43). The slides were washed with buffer (PBS, 5% sheep serum, 0.1% azide, 1 mM $MgCl_2$, 1 mM $CaCl_2$) and blocked with 20% sheep serum in PBS. The slides were treated with LEL followed by avidin-fluorescein (Southern Biotech, Birmingham, AL) or avidin-fluorescein alone as a control. The slides were incubated for 1 h at 21°C, washed three times, and mounted with DAPI-containing medium (Vector Laboratories. Burlingame, CA).

Fluorescence microscopy

The tissue sections were imaged with a Nikon Eclipse TE2000 inverted epifluorescence microscope by using Nikon objectives of 10× and 20× linear magnification with infinity correction. An X-Cite™ (Exfo, Vanier, Quebec, Canada) 120 W metal halide light source and a liquid light guide were used to illuminate the tissue samples. The excitation and emission filters (Chroma Technology, Bellows Falls, VT) were controlled by an MAC5000 controller (Ludl, Hawthorne, NY) and MetaMorph® software 7.8 (Molecular Devices, Downington, PA). The fluorescence microscopy 16-bit fluorescent images were recorded on a C9100-02 camera (Hamamatsu, Japan), digitally recombined, and pseudocolored based on recording wavelength. Nuclear staining with DAPI (Vector Laboratories), ethidium (Sigma-Aldrich), and Hoechst 33342 (Sigma) were used to evaluate the monolayer.

Pectins

The pectins used in this study were commercially obtained (Cargill, Minneapolis, MN). The proportion of galacturonic acid residues in the methyl ester form determined the degree of methoxylation. HMP were defined as those pectins with a degree of methoxylation >50%; low-methoxyl pectins were defined as those pectins with a degree of methoxylation <50%. The low-methoxyl pectins were also tested as non-amidated (LMC) and amidated (LMA) variants.

Load/displacement measurements

Load/displacement measurements were made by using an apparatus customized for tissue application. Loads were applied at comparable rates; tissue displacement was digitally recorded and analyzed by MetaMorph 7.8 morphometry software (Molecular Devices, Downington, PA). For all three bioadhesion tests, the pectin mixtures provided a rigid interface on which the tissue adherend was applied. The forces were applied to the various tissues with a Prolene suture (Ethicon, Somerville, NJ) passed through the tissue within 2 mm of the adhesive interface. All three tests were performed with uniaxial load application; all loads were applied to uniform cross-sectional areas of bioadhesion. Adhesion development time was comparable for all specimens; all tests were performed after warming samples to near 37°C. Tensile strength was tested at a 90^{o} load application, peel strength was tested at a 120^{o} angle of separation, and shear resistance was tested by forces that were applied parallel to the adhesive interface.

Enzyme treatment

The tissues were treated with three commercially obtained enzymes previously used to treat mesothelium[20] (Sigma-Aldrich, St. Louis, MO): Hyaluronidase cleaved the $1 \rightarrow 4$ linkages between N-acetyl-D-glucosamine and D-glucuronate; neuraminidase, also called sialidase, cleaved the glycosidic linkages of neuraminic acids; and pronase is a mixture of proteases derived from Streptomyces griseus.

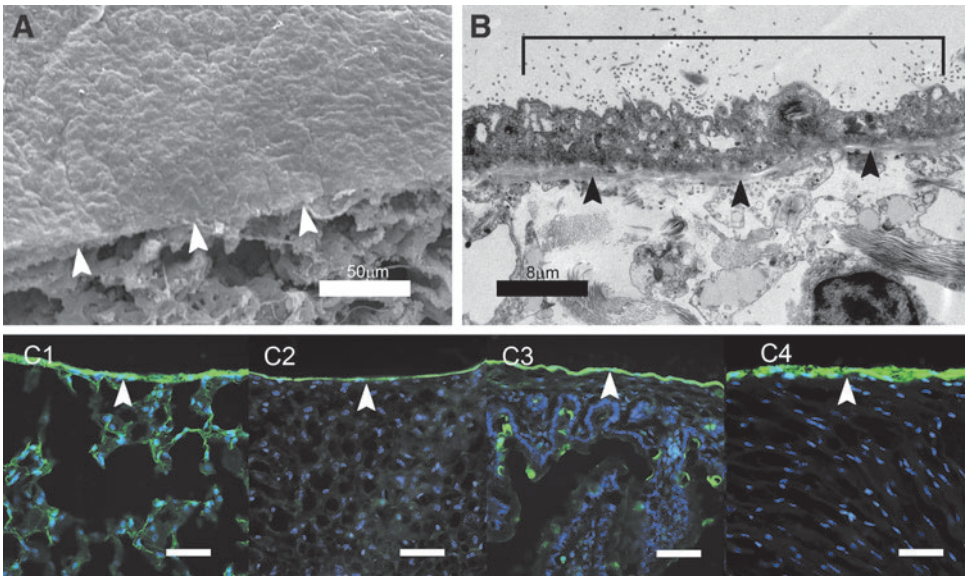

FIG. 1. Murine visceral mesothelium and glycocalyx. **(A)** Scanning electron micrograph of the murine lung visceral pleura. The ''flagstone'' appearance of the mesothelium was demonstrated above the cut surface of the lung (*arrows*). **(B)** TEM of the visceral pleural mesothelium demonstrated microvilli (*bracket*) and the underlying mesothelial basement membrane (*black arrows*). The intervillar glycocalyx was not seen in TEM. **(C)** Staining visceral mesothelium with the *green* fluorescent LEL (Vector Laboratories) demonstrated the glycocalyx (*arrows*) in the lung (C1), liver (C2), bowel (C3), and heart (C4). The *blue* nuclei reflected Hoechst 33342 (Sigma) counterstain. Scale bars = 60 µm. LEL, Lycopersicon esculentum lectin; TEM, transmission electron microscopy.

Enzyme solutions and tissues were maintained at 37°C during either a 5 min (pronase) or 90-min incubation (hyaluronidase and neuraminidase). After enzyme treatment, the tissues were washed with PBS three times.

Silver nitrate staining

The pleural mesothelium was washed with a glucose solution (50 mg/mL) for 3 min, exposed to 0.4 mg/mL silver nitrate *in situ* for 30 s followed by another 3-min wash with the glucose solution. The tissue was exposed to UV light for 30 s. After brief drying with Argon gas, the pleural was mounted and staining was performed as described by Lee *et al.*[21]

Statistics

Statistical analyses were based on measurements in at least three different specimens. The unpaired Student's *t*-test

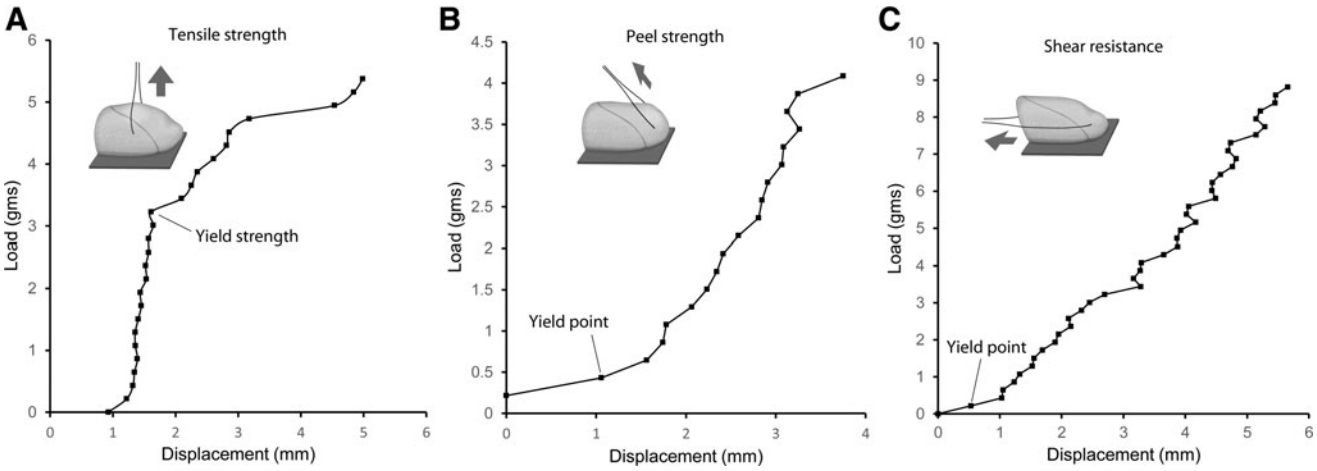

FIG. 2. Load/displacement measurements. The adhesion of mesothelium to the pectin-based bioadhesive was assessed by three factors: **(A)** tensile strength, **(B)** peel strength, and **(C)** shear resistance. The tissue was applied—with ~0.1 N force and 3–5 min development time—to the firm pectin-based substratum that was composed of 50% pectin and 50% CMC. Loads were applied at a controlled rate to a suture passed through the tissue within 2 mm of the adhesive interface. The lung demonstrated tensile strength **(A)** greater than peel strength **(B)** or shear resistance **(C)**. The adhesion of lung to equal weight % pectin and CMC is shown. Notably, peel and shear forces applied to the lung demonstrated near-interface parenchymal separation (yield point) that facilitated the isolation of the pleural mesothelium. The results represent median values of $N = 5$ replicates. CMC, carboxymethylcellulose.

for samples of unequal variances was used to calculate statistical significance. The data were expressed as mean ± one standard deviation. The significance level for the sample distribution was defined as $p < 0.05$.

Results

Visceral mesothelium

Mesothelium has a characteristic ''flagstone'' appearance by scanning electron microscopy (SEM) (Fig. 1A). Transmission electron microscopy (TEM) demonstrated that free surface of the mesothelium was covered by microvilli (Fig. 1B, bracket); the basal layer was delimited by a discrete basement membrane (Fig. 1B, arrows). The mesothelial glycocalyx was not visible by using electron microscopy; however, fluorescent lectin staining demonstrated a prominent glycocalyx expressed on the free surface of the lung, liver, bowel, and heart mesothelium (Fig. 1C).

Mesothelial bioadhesion

Based on previous mucoadhesion studies,[22] a pectin and carboxymethylcellulose (CMC) equal weight % mixture was used to screen for mesothelial adhesion. Uniform and malleable, the lung was used for initial adhesion studies. The lung visceral pleura was applied to the pectin-CMC substratum for a 3-min development period. The interface was subsequently tested for tensile strength, peel strength (120°), and shear resistance (Fig. 2). The tensile force required to disrupt the pectin-lung interface (yield strength) was more than 6-fold greater than the comparable displacement produced by the peel force and shear force (Fig. 2). An interesting observation was the near-interface structural

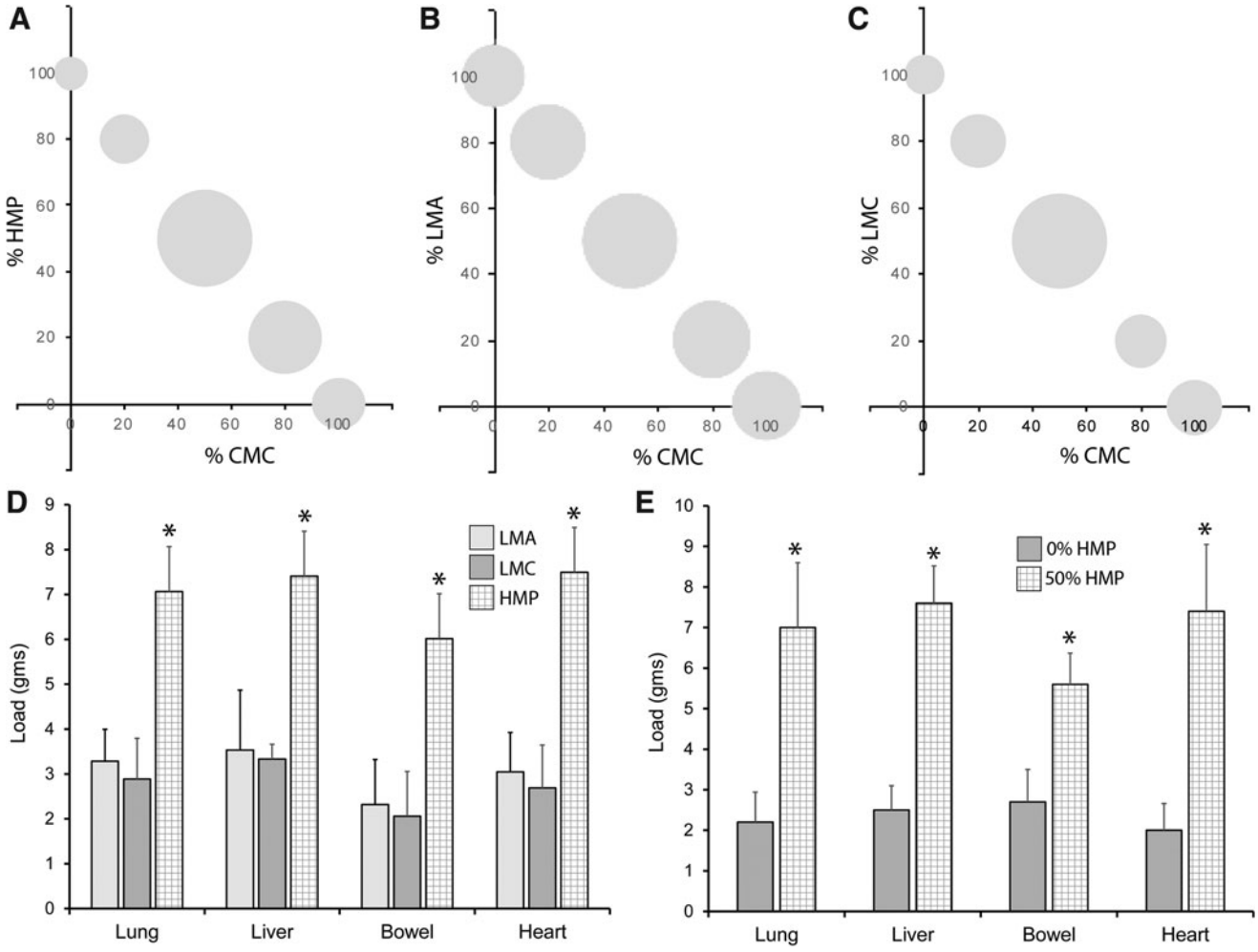

FIG. 3. Tensile strength of visceral mesothelium adhesion to varied mixtures of pectin and CMC. **(A–C)** The adhesion strength of CMC and different weight ratios of HMP, amidated low-methoxyl (LMA), and nonamidated low-methoxyl (LMC) pectin were tested for relative tensile strength; liver adhesion is shown. The area of the bubble reflects relative adhesion strength of the different mixtures scaled to 100. The greatest adhesion strength was demonstrated in equal weight (%) ratio of all three pectins and CMC. **(D)** Comparison of adhesion strength of HMP, LMA, and LMC and equal weight (%) ratio mixtures of CMC tested against all 4 mesothelial tissues. HMP demonstrated consistently greater adhesion than comparable LMA and LMC pectin (*asterisk*, $p < 0.05$). **(E)** Comparison of equal weight ratio of HMP and CMC (50%) and CMC with no pectin (0%) for all four mesothelial tissues. The 50% mixture was significantly greater than the 0% mixture for all four tissues (*asterisk*, $p < 0.05$). Error bars = 1 SD of triplicate samples. LMA, amidated low-methoxyl; HMP, high-methoxyl pectin; SD, standard deviation.

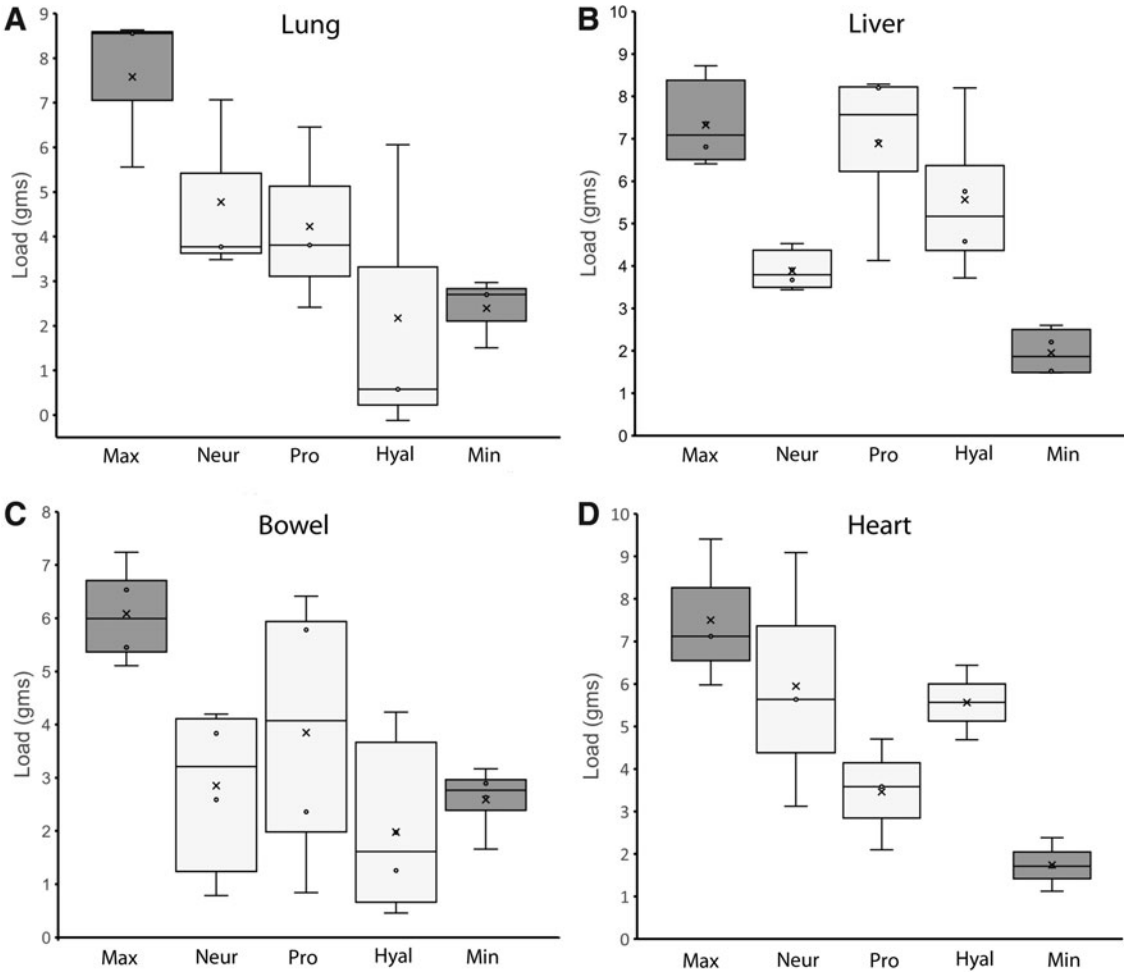

FIG. 4. Bioadhesion of visceral mesothelium after pretreatment with glycocalyx-directed enzymes. The lung **(A)**, liver **(B)**, bowel **(C)**, and heart **(D)** tissue was treated with neuraminidase (Neur), pronase (Pro), or hyaluronidase (Hyal) at established concentrations[20] before adhesion on a 50% HMP and CMC substratum. The 50% HMP (Max) and 0% pectin (Min) provided control comparisons for the enzyme effects on tensile strength. Tensile strength was diminished by all three enzymes; however, a significant quantitative variation in enzyme inhibition was noted. Box plots indicate median values and 25th and 75th percentile; *whiskers* represent variability outside the upper and lower quartiles. Data represent replicate samples of $N=3$ mice.

failure of the lung parenchyma when exposed to progressive peel and shear force (yield point, Fig. 2B, C).

To determine the optimal composition of the pectin adhesive, three types of pectin—low-methoxyl (LMC), amidated low-methoxyl (LMA), and HMP—were tested with varying concentrations of CMC. When tested on liver mesothelium, all three pectin formulations demonstrated maximum adhesion with an equal weight ratio (%) with CMC (Fig. 3A–C). For all four mesothelial tissues, HMP consistently demonstrated greater adhesivity than either LMC or LMA pectin ($p<0.05$) (Fig. 3D). The quantitative contribution of HMP to mesothelial adhesion was demonstrated when an equal weight% of HMP and CMC (50%) was compared with CMC alone (0%) (Fig. 3E). The equal weight mixture of HMP and CMC demonstrated significantly greater adhesive strength ($p<0.05$) (Fig. 3E).

Glycocalyx dependence

To test the dependence of pectin bioadhesion on the mesothelial glycocalyx, we treated the mesothelial tissues with hyaluronidase, pronase, and neuraminidase.[20] The enzyme-treated mesothelium demonstrated diminished tensile strength of the pectin-based adhesion (Fig. 4). The average reduction of pectin adhesion was lung 58%±17%, liver 35%±27%, bowel 85%±29%, and heart 37%±31%. The variable efficacy of the different enzyme treatments suggested structural differences in the mesothelial glycocalyces of the four tissues.

Near-interface separation

In the assessment of lung adhesion, peel and shear resistance at the lung/pectin adhesive interface was associated with structural ''failure'' in the subjacent lung (yield point, Fig. 2). The parenchymal separation occurred in the subpleural alveoli. Assisted by limited blunt dissection, combined shear and peel forces removed the bulk of the lung parenchyma, leaving a 30–50 μm thick layer with an intact basement membrane adherent to the pectin. With hydration, the separated mesothelial layer was ''floated off'' the pectin adhesive, leaving an en face preparation (Fig. 5A). The en

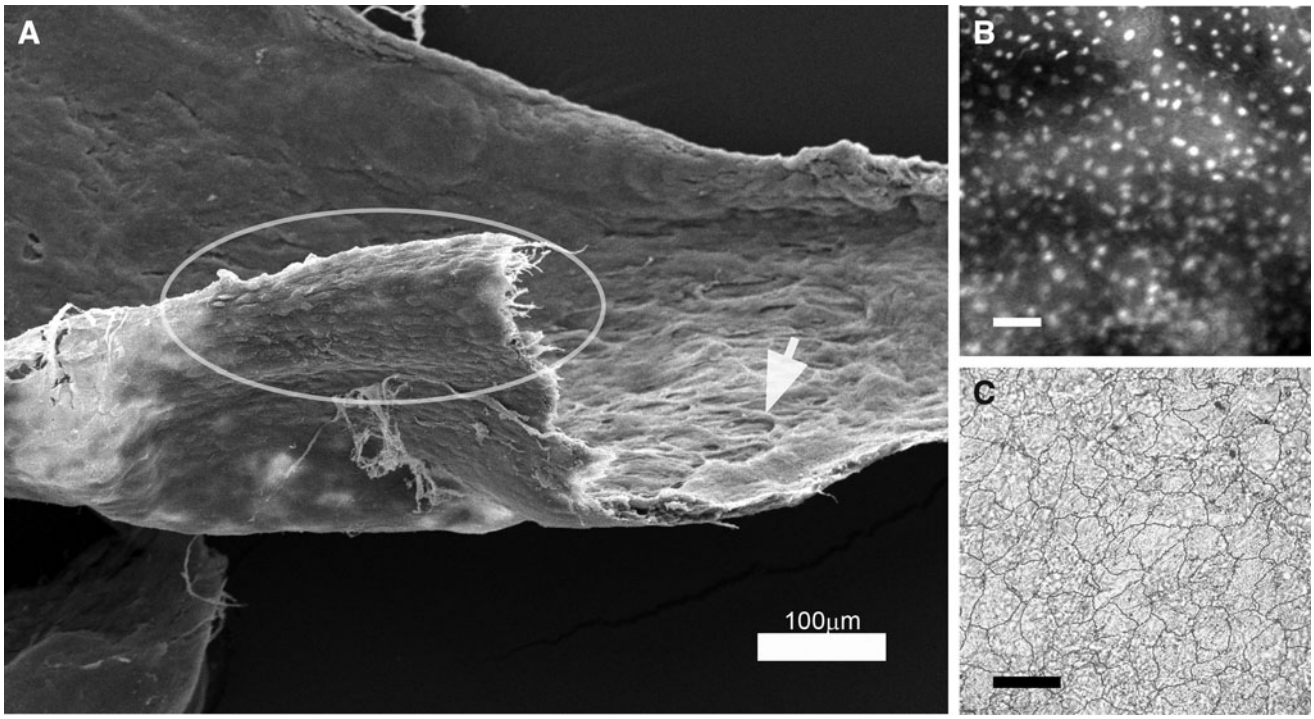

FIG. 5. Shear and peel force isolation of en face pleural mesothelium. A combination of shear force and peel force applied to the lung-pectin adhesion resulted in the separation of the mesothelium from the subjacent lung. **(A)** SEM of the resulting mesothelial layer showed the typical ''flagstone'' appearance of the free surface of the mesothelium (ellipse) and alveolar remnants on the deep surface of the layer (*arrow*). **(B)** Fluorescent nuclear staining demonstrated an intact monolayer (scale bar = 100 μm). **(C)** Silver staining demonstrated intact tight junctions (scale bar = 50 μm). SEM, scanning electron microscopy.

face layer was a continuous monolayer (Fig. 5B) with intact tight junctions by silver staining (Fig. 5C).

Discussion

In this article, we defined four features of the bioadhesive interaction between pectin biopolymers and the glycocalyx of visceral mesothelium. (1) An equal weight % mixture of pectin and CMC demonstrated significant tensile strength in adhesion to the lung, liver, bowel, and heart mesothelium. (2) HMP demonstrated greater adhesivity than low-methoxyl or amidated low-methoxyl pectin compounds. (3) Consistent with a mechanism of polysaccharide-dependent adhesion, pectin binding was diminished by enzyme treatment. (4) Shear force applied to the pectin/lung adhesion resulted in near-interface structural failure—a reproducible observation that facilitated the selective isolation of the mesothelial layer of the lung. We conclude that pectins bind the mesothelial glycocalyx, likely through a mechanism of interpenetration, providing a potentially useful tool in experimental and therapeutic manipulations of the lung, liver, bowel, and heart mesothelium.

The adhesion measurements performed in this work were necessarily a modification of existing adhesion testing methods.[23] In most industrial methods,[24,25] adhesion is the strength of the bond between the adherend (e.g., tape) and the substratum (application surface). In this application, the adherend was biological tissue and the substratum was the pectin-based polymer. Unable to usefully distinguish the relative contributions of the tissue, the adhesive bond, and the pectin-based substratum, we empirically defined adhesive strength as the load at which tissue-substratum separation occurred. Tensile strength, peel adhesion, and shear resistance simply reflected the direction of the applied load. The validity of this approach was suggested by the reproducible and discriminating measures of pectin-based polymer adhesion to the lung, liver, bowel, and heart. Further, adhesive strength appeared to reflect polysaccharide-dependent adhesion as tensile strength was notably influenced by pectin concentration, pectin chemistry, and enzyme pretreatment.

The mesothelial binding of the pectin-based adhesives in this study suggests several potential applications of these compounds in tissue engineering, wound healing, and drug delivery. Although biopolymers, such as albumin-based Progel (Bard Davol, Murray Hill, NJ), are currently used to treat pleural injury (''air leaks'') after pulmonary surgery,[26] their effectiveness has been limited by poor adhesivity to the pleura.[27] In contrast to these polypeptide polymers, pectin-based compounds offer the potential for tight binding to the mesothelial glycocalyx. In addition to providing a scaffold for mesothelial regeneration, pectin-based compounds could facilitate the delivery of drugs or growth factors to the mesothelial surface. Another potential target for mesothelial treatment is the inhibition of post-treatment serosal adhesions that often lead to bowel obstruction in the peritoneum,[28] impaired lung function in the pleura,[29] and compromised heart function in the pericardium.[30]

A common constituent of plant cell walls, pectin is a structural heteropolysaccharide that is cell friendly and of a low cost, specifically, features that have led to an interest in

pectin as a mucoadhesive for gut drug delivery.[14] Pectins can vary in molecular weight, cross-linking density, and chemical groups (e.g., hydroxyl, amine, sulfur, and carboxyl groups).[31–33] Our selection of pectin-based adhesives was empirical; that is, the HMP demonstrated efficient and reversible adhesivity.

In the lung, the shear-induced subpleural structural failure and the reversibility of the pectin-based bioadhesives were unique properties that facilitated the isolation of visceral pleural mesothelium and preserved the en face monolayer relationships that exist *in situ*. Similar structural failure was not observed in the liver, bowel, and heart. The use of pectin-based adhesion to isolate intact mesothelium represents a significant advance over previous methods. Previous Hautchen (''thin skin'') en face monolayer preparation techniques have largely focused on the isolation of endothelial cells.[34] These methods have involved surgical dissection,[35] fixation to a metal frame,[36–39] fixation to glass slides,[40–42] as well as adherence to collodion[43–45] and tape.[34] With few exceptions, the technical limitations were unpredictable cell loss, incomplete stripping, disruption of the monolayer, and wrinkling of the specimen. In contrast, the use of the pectin-based compounds in this study resulted in largely intact en face monolayers associated with minimal cell loss.

Finally, the observations in this article reflect the properties of the mesothelial glycocalyx. The word glycocalyx (Greek, ''sweet husk'') was coined to provide a more general term for the extracellular polysaccharide-rich coatings of many eukaryotic and prokaryotic cells.[46] Andrews and Porter[47] used ruthenium red and TEM to demonstrate a glycocalyx coating the microvilli and intervillar surfaces of many tissues, including the lung, liver, bowel, and heart mesothelium. In the pleural, pericardial, and peritoneal mesothelium, cytochemical techniques have demonstrated a 28–57 nm thick glycocalyx coating the cell surface and intervillar regions.[48,49] Enzyme treatments with hyaluronidase and neuraminidase suggest that the pleural mesothelial glycocalyx is composed of sialic acid residues and other mucoproteins.[50] Similarly, cationic colloidal iron staining suggests that the glycocalyx consists of negatively charged sialomucins on the surface of the pleural, pericardial, and peritoneal mesothelium.[49] The function of the mesothelial glycocalyx is uncertain, but primary functions likely include the maintenance of epithelial hydration and the minimization of frictional forces.[51] Pectin-based bioadhesives provide a useful tool to elucidate the structure and function of the mesothelial glycocalyx.

Acknowledgments

This study was supported, in part, by NIH Grants HL94567, HL007734, HL134229, CA009535, and ES000002.

Disclosure Statement

No competing financial interests exist.

References

1. Schnepp, Z. Biopolymers as a flexible resource for nanochemistry. Angew Chem Int Ed Engl **52,** 1096, 2013.
2. Garcia-Gonzalez, C.A., Alnaief. M., Smirnova, I. Polysaccharide-based aerogels-Promising biodegradable carriers for drug delivery systems. Carbohydr Polym **86,** 1425, 2011.
3. Malafaya, P.B., Silva, G.A., Reis, R.L. Natural-origin polymers as carriers and scaffolds for biomolecules and cell delivery in tissue engineering applications. Adv Drug Deliv Rev **59,** 207, 2007.
4. Shachar, M., Tsur-Gang, O., Dvir, T., Leor, J., Cohen, S. The effect of immobilized RGD peptide in alginate scaffolds on cardiac tissue engineering. Acta Biomater **7,** 152, 2011.
5. Khanarian, N.T., Haney, N.M., Burga, R.A., Lu, H.H. A functional agarose-hydroxyapatite scaffold for osteochondral interface regeneration. Biomaterials **33,** 5247, 2012.
6. Pooyan, P., Tannenbaum, R., Garmestani, H. Mechanical behavior of a cellulose-reinforced scaffold in vascular tissue engineering. J Mech Behav Biomed Mater **7,** 50, 2012.
7. Kumar, P.T.S., Srinivasan, S., Lakshmanan, V.-K., Tamura, H., Nair, S.V., Jayakumar, R. beta-Chitin hydrogel/nano hydroxyapatite composite scaffolds for tissue engineering applications. Carbohydr Polym **85,** 584, 2011.
8. Coimbra. P., Ferreira, P., de Sousa, H.C., Batista, P., Rodrigues, M.A., Corriea, I.J., *et al.* Preparation and chemical and biological characterization of a pectin/chitosan polyelectrolyte complex scaffold for possible bone tissue engineering applications. Int J Biol Macromol **48,** 112–118, 2011.
9. Scheller, H.V., Jensen, J.K., Sorensen, S.O., Harholt, J., Geshi, N. Biosynthesis of pectin. Physiol Plant **129,** 283, 2007.
10. Monsoor, M.A., Kalapathy, U., Proctor, A. Determination of polygalacturonic acid content in pectin extracts by diffuse reflectance Fourier transform infrared spectroscopy. Food Chem **74,** 233, 2001.
11. Nunes, C., Silva, L., Fernandes, A.P., Guine, R.P.F., Domingues, M.R.M., Coimbra, M.A. Occurrence of cellobiose residues directly linked to galacturonic acid in pectic polysaccharides. Carbohydr Polym **87,** 620, 2012.
12. Munarin, F., Guerreiro, S.G., Grellier, M.A., Tanzi, M.C., Barbosa, M.A., Petrini, P., *et al.* Pectin-based injectable biomaterials for bone tissue engineering. Biomacromolecules **12,** 568, 2011.
13. Smistad, G., Boyum, S., Alund, S.J., Samuelsen, A.B.C., Hiorth, M. The potential of pectin as a stabilizer for liposomal drug delivery systems. Carbohydr Polym **90,** 1337, 2012.
14. Munarin, F., Tanzi, M.C., Petrini, P. Advances in biomedical applications of pectin gels. Int J Biol Macromol **51,** 681, 2012.
15. Edsman, K., Hagerstrom, H. Pharmaceutical applications of mucoadhesion for the non-oral routes. J Pharm Pharmacol **57,** 3, 2005.
16. VanTeeffelen, J.W., Brands, J., Stroes, E.S., Vink, H. Endothelial glycocalyx: sweet shield of blood vessels. Trends Cardiovasc Med **17,** 101, 2007.
17. Bodega, F., Sironi, C., Porta, C., Zocchi, L., Agostoni, E. Pleural mesothelium lubrication after phospholipase treatment. Respir Physiol Neurobiol **194,** 49, 2014.
18. Gibney, B., Lee, G.S., Houdek, J., Lin, M., Chamoto, K., Konerding, M.A., *et al.* Dynamic determination of oxygenation and lung compliance in murine pneumonectomy. Exp Lung Res **37,** 301, 2011.
19. Nachbar, M.S., Oppenheim, J.D., Thomas, J.O. Lectins in the U.S. Diet. Isolation and characterization of a lectin from the tomato (Lycopersicon esculentum). J Biol Chem **255,** 2056, 1980.
20. Sironi, C., Bodega, F., Porta, C., Agostoni, E. Pleural mesothelium lubrication after hyaluronidase, neuraminidase or pronase treatment. Respir Physiol Neurobiol **188,** 60, 2013.

21. Lee, Y.U., Drury-Stewart, D., Vito, R.P., Han, H.C. Morphologic adaptation of arterial endothelial cells to longitudinal stretch in organ culture. J Biomech **41,** 3274, 2008.
22. Singh, I., Rana, V. Techniques for the assessment of mucoadhesion in drug delivery systems: an overview. J Adhes Sci Technol **26,** 2251, 2012.
23. Volume 15.06 Adhesives. Annual Book of ASTM Standards. West Conshohocken, PA: ASTM International; 2017.
24. Ebnesajjad, S., Landrock, A.H. Adhesives Technology Handbook. 3rd ed. Amsterdam: Elsevier; 2015.
25. Benedek, I. Pressure-Sensitive Adhesives and Applications. 2nd ed. CRC Press; 2004.
26. Fuller, C. Reduction of intraoperative air leaks with Progel in pulmonary resection: a comprehensive review. J Cardiothorac Surg **8,** 90, 2013.
27. Malapert, G., Abou Hanna, H., Pages, P.B., Bernard, A. Surgical sealant for the prevention of prolonged air leak after lung resection: meta-analysis. Ann Thorac Surg **90,** 1779, 2010.
28. Brochhausen, C., Schmitt, V.H., Rajab, T.K., Planck, C.N.E., Kraemer, B., Wallwiener, M., *et al.* Intraperitoneal adhesions-An ongoing challenge between biomedical engineering and the life sciences. J Biomed Mater Res Part A **98A,** 143, 2011.
29. Loring, S.H., Kurachek, S.C., Wohl, M.E. Diaphragmatic excursion after pleural sclerosis. Chest **95,** 374, 1989.
30. Troughton, R.W., Asher, C.R., Klein, A.L. Pericarditis. Lancet **363,** 717, 2004.
31. Robert, C., Buri, P., Peppas, N.A. Experimental-method for bioadhesive testing of various polymers. Int J Drug Formul Biopharm **34,** 95, 1988.
32. Duchene, D., Touchard, F., Peppas, N.A. Pharmaceutical and medical aspects of bioadhesive systems for drug administration. Drug Dev Ind Pharm **14,** 283, 1988.
33. Leung, S.H.S., Robinson, J.R. Polymer structure features contributing to mucoadhesion. II. J Control Release **12,** 187, 1990.
34. Hirsch, E.Z., Martino, W., Orr, C.H., White, H., Chisolm, G.M. A simple rapid method for the preparation of en-face endothelial (hautchen) monolayers from rat and rabbit aortas. Atherosclerosis **37,** 539, 1980.
35. Zahn, F.W. Versuchung über die vernarbung von querrissen der arterienintima und media nach vorheriger umschnürung. Virchows Arch Pathol Anat Physiol Klin Med **96,** 1, 1884.
36. O'Neill, J.F. The effects on venous endothelium of alterations in blood flow through the vessels in vein walls, and the possible relation to thrombosis. Ann Surg **126,** 270, 1947.
37. Samuels, P.B., Samuels, B.M., Webster, D.R. New technics in the study of venous endothelium. Lab Investig **1,** 50, 1952.
38. Lautsch, E.V, McMillan, G.C., Duff, G.L. Technics for the study of the normal and atherosclerotic arterial intima from its endothelial surface. Lab Investig **2,** 397, 1953.
39. Poole, J.C.F, Sanders, A.G., Florey, H.W. The regeneration of aortic endothelium. J Pathol Bacteriol **75,** 133, 1958.
40. Sade, R.M., Folkman, J. En face stripping of vascular endothelium. Microvasc Res **4,** 77, 1972.
41. Riese. K.H., Freudenberg, N., Haas, W. En face preparation methods for investigation of endothelia and mesothelia. Pathol Res Pract **162,** 327, 1978.
42. Jelev, L., Surchev, L. A novel simple technique for en face endothelial observations using water-soluble media – ''thinned-wall'' preparations. J Anat **212,** 192, 2008.
43. Sinapius, D. Uber das aortenendothel. Virchows Arch Pathol Anat Physiol Klin Med **322,** 662, 1952.
44. Eskeland, G., Kjaerheim A. Regeneration of parietal peritoneum in rats. 1. A light microscopical study. Acta Pathol Microbiol Scand **68,** 355, 1966.
45. Schwartz, S.M., Benditt, E.P. Cell replication in aortic endothelium - new method for study of problem. Lab Investig **28,** 699, 1973.
46. Bennett, H.S. Morphological aspects of extracellular polysaccharides. J Histochem Cytochem **11,** 14, 1963.
47. Andrews, P.M., Porter, K.R. Ultrastructural morphology and possible functional significance of mesothelial microvilli. Anat Rec **177,** 409, 1973.
48. Schwarz, W. Surface film on mesothelium of serous membranes of rat. Z Zellforsch Mikrosk Anat **147,** 595, 1974.
49. Ohtsuka, A., Yamana, S., Murakami, T. Localization of membrane-associated sialomucin on the free surface of mesothelial cells of the pleura, pericardium, and peritoneum. Histochem Cell Biol **107,** 441, 1997.
50. Wang, N.S. Regional difference of pleural mesothelial cells in rabbits. Am Rev Respir Dis **110,** 623, 1974.
51. Bodega, F., Sironi, C., Porta, C., Pecchiari, M., Zocchi, L., Agostoni, E. Mixed lubrication after rewetting of blotted pleural mesothelium. Respir Physiol Neurobiol **185,** 369, 2013.

Address correspondence to:
Steven J. Mentzer, MD
Laboratory of Adaptive and Regenerative Biology
Brigham and Women's Hospital
Harvard Medical School
Room 259, 75 Francis Street
Boston, MA 02115

E-mail: smentzer@bwh.harvard.edu

Received: January 23, 2017
Accepted: April 25, 2017
Online Publication Date: June 30, 2017